Supporting Information For

Theoretical Study of Electronic Structure and Chemical Bonding in MOB^- and MBO^- (M = Sc – Zn) Molecules

Ze-Hui Wang[a,b], Xue-Lian Jiang[b], Xiaohu Yu[a], Tianlei Zhang[a*], Jun Li[c,d], Cong-Qiao Xu[b*]

[a] Shaanxi Key Laboratory of Catalysis, Institute of Theoretical and Computational Chemistry, Shaanxi University of Technology, Hanzhong 723000, China

[b] Department of Chemistry, Southern University of Science and Technology, Shenzhen 518055, China

[c] Department of Chemistry and Engineering Research Center of Advanced Rare-Earth Materials of Ministry of Education, Tsinghua University, Beijing 100084, China

[d] Fundamental Science Center of Rare Earths, Ganjiang Innovation Academy, Chinese Academy of Sciences, Ganzhou 341000, China

* Corresponding authors: ztianlei88@163.com, xucq@sustech.edu.cn

KEYWORDS boronyl ligand • transition metal complex • electronic structure • chemical bonding • periodic trend

Table S1. Valence electronic configurations and orbital compositions of CO and BO molecules, based on the energy level and irreducible representation shown in Figure 1.

	Valence configuration		Valence configuration
BO	$2\pi^0$(83.12%B + 16.88%O)	CO	$2\pi^0$(77.97%C + 22.03%O)
	$5\sigma^1$(86.74%B + 13.26%O)		$5\sigma^2$(90.98%C + 9.02%O)
	$1\pi^4$(80.43%O + 19.57%B)		$1\pi^4$(73.89%O + 26.11%C)
	$4\sigma^2$(81.46%O + 18.55%B)		$4\sigma^2$(80.60%O + 19.40%C)
	$3\sigma^2$(84.66%O + 15.34%B)		$3\sigma^2$(76.09%O + 23.91%C)

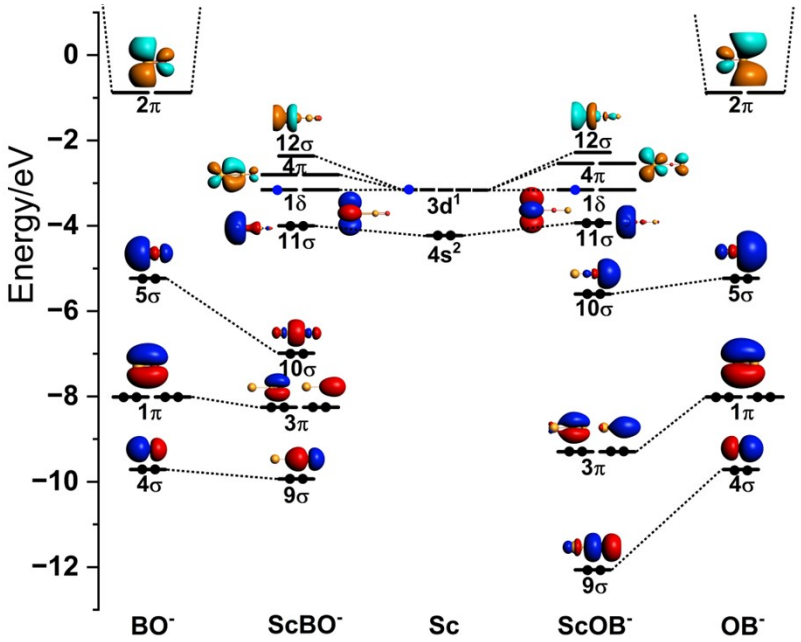

Figure S1. Molecular orbital (MO) energy levels of $Sc(OB)^-$ and $Sc(BO)^-$ calculated at the PBE/TZ2P level, based on geometries optimized at the CCSD(T)/def2-TZVP level.

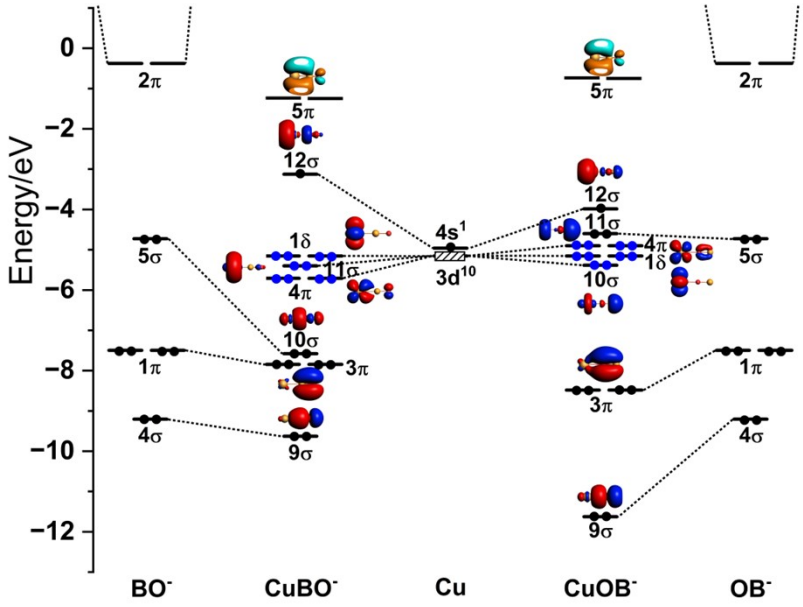

Figure S2. Molecular orbital (MO) energy levels of $Cu(OB)^-$ and $Cu(BO)^-$ calculated at the PBE/TZ2P level, based on geometries optimized at the CCSD(T)/def2-TZVP level.

Table S2. The electron configurations of $M(OB)^-$ and $M(BO)^-$ (M = Sc - Zn) at the PBE/TZ2P level (All energies in kcal/mol). The ground states are highlighted in bold.

M(BO)$^-$	2s + 1	Configuration	Energy	M(OB)$^-$	2s + 1	Configuration	Energy
	2	**a. π^1**	**-360.81**		2	a. π^1	-360.92
Sc(BO)$^-$	2	b. δ^1	-358.24	Sc(OB)$^-$	**2**	**b. δ^1**	**-364.55**
	2	c. σ^1	-350.13		2	c. σ^1	-354.2
	3	**a. π^2**	**-385.78**		3	a. π^2	-378.91
Ti(BO)$^-$	3	b. δ^2	-378.95	Ti(OB)$^-$	3	b. δ^2	-383.52
	3	c. σ^2	-315.94		3	c. σ^2	-317.2
	3	d. $\pi^1\sigma^1$	-385.48		**3**	**d. $\pi^1\sigma^1$**	**-383.76**
	2	a. $\sigma^2\delta^1$	-406.27		2	a. $\sigma^2\delta^1$	-390.94
	2	b. $\sigma^2\pi^1$	-307.27		2	b. $\sigma^2\pi^1$	-306.39
	4	c. $\pi^2\delta^1$	-423.55		4	c. $\pi^2\delta^1$	-409.75
V(BO)$^-$	4	d. $\delta^2\pi^1$	-414.54	V(OB)$^-$	4	d. $\delta^2\pi^1$	-410.76
	4	e. $\pi^2\sigma^1$	-375.79		4	e. $\pi^2\sigma^1$	-369.98
	4	f. $\delta^2\sigma^1$	-393.77		4	f. $\delta^2\sigma^1$	-397.53
	6	**g. $\pi^2\delta^2$**	**-425.66**		**6**	**g. $\pi^2\delta^2$**	**-415.59**
	1	a. π^4	-375.69		1	a. π^4	-345.22
	1	b. δ^4	-334.85		1	b. δ^4	-334.73
	3	c. $\pi^2\sigma^2$	-316.07		3	c. $\pi^2\sigma^2$	-313.53
Cr(BO)$^-$	3	d. $\delta^2\sigma^2$	-365.98	Cr(OB)$^-$	3	d. $\delta^2\boldsymbol{\sigma}^2$	-368.43
	5	e. $\pi^2\delta^2$	-470.25		5	e. $\pi^2\delta^2$	-458.70
	7	**f. $\pi^2\delta^2\sigma^1$**	**-472.27**		**7**	**f. $\pi^2\delta^2\sigma^1$**	**-461.11**
	2	a. $\pi^4\sigma^1$	-320.55		2	a. $\pi^4\sigma^1$	-299.65
	2	b. $\delta^4\sigma^1$	-347.50		2	b. $\delta^4\sigma^1$	-345.46
	2	c. $\pi^4\sigma^2$	-274.76		2	c. $\pi^4\sigma^2$	-253.07
Mn(BO)$^-$	2	d. $\delta^4\sigma^2$	-308.79	Mn(OB)$^-$	2	d $\delta^4\sigma^2$	-314.05
	6	**e. $\pi^2\delta^2\sigma^1$**	**-472.77**		**6**	**e. $\pi^2\delta^2\sigma^1$**	**-468.32**
	6	f. $\pi^2\delta^2\sigma^2$	-437.80		6	f. $\pi^2\delta^2\sigma^2$	-426.40
	1	a. $\pi^4\sigma^2$	-308.3		1	a. $\pi^4\sigma^2$	-216.96
	1	b. $\delta^4\sigma^2$	-220.61		1	b. $\delta^4\sigma^2$	-314.21
	3	**c. $\pi^2\delta^4$**	**-452.55**		3	c. $\pi^2\delta^4$	-398.57
Fe(BO)$^-$	3	d. $\pi^4\delta^2$	-412.58	Fe(OB)$^-$	**3**	**d. $\pi^4\delta^2$**	**-419.11**
	5	e. $\pi^2\delta^2\sigma^2$	-417.21		5	e. $\pi^2\delta^2\sigma^2$	-415.44
	5	f. $\delta^4\pi^2\sigma^1$	-413.02		5	f. $\delta^4\pi^2\sigma^1$	-403.25
	5	g. $\delta^2\pi^4\sigma^1$	-444.64		5	g. $\delta^2\pi^4\sigma^1$	-415.73
	2	**a. $\pi^4\delta^3$**	**-437.60**		2	a. $\pi^4\delta^3$	-402.81
	2	b. $\delta^4\pi^3$	-415.58		2	b. $\delta^4\pi^3$	-389.52
	2	c. $\pi^4\delta^4$	-405.62		2	e. $\pi^4\delta^4$	-367.59
Co(BO)$^-$	4	d. $\delta^4\pi^2\sigma^1$	-419.5	Co(OB)$^-$	**4**	**d. $\delta^4\pi^2\sigma^1$**	**-408.98**
	4	e. $\pi^4\delta^2\sigma^1$	-424.95		4	c. $\pi^4\delta^2\sigma^1$	-399.96
	4	f. $\delta^4\pi^2\sigma^2$	-375.42		4	f. $\delta^4\pi^2\sigma^2$	-375.9
	4	g. $\delta^2\pi^4\sigma^2$	-382.46		4	g. $\delta^2\pi^4\sigma^2$	-366.99
	1	**a. $\pi^4\delta^4$**	**-398.26**		**1**	**a. $\pi^4\delta^4$**	**-358.65**
	3	b. $\pi^4\delta^2\sigma^2$	-295.69		3	b. $\pi^4\delta^2\sigma^2$	-292.52
	3	c. $\delta^4\pi^2\sigma^2$	-325.27		3	c. $\delta^4\pi^2\sigma^2$	-325.51
Ni(BO)$^-$	3	d. $\pi^4\delta^3\sigma^1$	-374.21	Ni(OB)$^-$	3	d. $\pi^4\delta^3\sigma^1$	-356.54
	3	e. $\pi^4\delta^4\sigma^1$	-376.52		3	e. $\pi^4\delta^4\sigma^1$	-353.98
	3	f. $\pi^4\delta^3\sigma^2$	-376.46		3	f. $\pi^4\delta^3\sigma^2$	-357.04

$Cu(BO)^-$	2	a. $\pi^4\delta^4\sigma^1$	-318.25	$Cu(OB)^-$	2	a. $\pi^4\delta^4\sigma^1$	/
	2	**b. $\pi^4\delta^4\sigma^2$**	**-369.98**		**2**	**b. $\pi^4\delta^4\sigma^2$**	**-345.18**
$Zn(BO)^-$	**1**	**a. $\pi^4\delta^4\sigma^2$**	**-323.69**	$Zn(OB)^-$	**1**	**a. $\pi^4\delta^4\sigma^2$**	**-320.95**

Table S3. The electron configurations of $M(OB)^-$ and $M(BO)^-$ (M = Sc - Zn) at the CCSD(T)/def2-TZVP level (All energies in kcal/mol). The ground states are highlighted in bold. [a]Entries marked with 'c' indicate that an orbital occupation adjustment was attempted using the ORCA program, but was unsuccessful.

$M(BO)^-$	2s + 1	Configuration	Energy	$M(OB)^-$	2s + 1	Configuration	Energy
$Sc(BO)^-$	2	a. π^1	37.65	$Sc(OB)^-$	**2**	**a. δ^1**	**-8.79**
	2	**b. δ^1**	**0.00**		/	/	/
$Ti(BO)^-$	3	a. π^2	/	$Ti(OB)^-$	**3**	**a. $\delta^1\pi^1$**	**-3.19**
	3	**b. $\delta^1\pi^1$**	**0.00**		3	b. π^2	0.00
$V(BO)^-$	6	a. $\pi^2\delta^2$	6.90	$V(OB)^-$	6	a. $\pi^2\delta^2$	12.55
	4	**b. $\pi^2\delta^1$**	**0.00**		**4**	**b. $\pi^2\delta^1$**	1.26
$Cr(BO)^-$	**7**	**a. $\pi^2\delta^2\sigma^1$**	**0.00**	$Cr(OB)^-$	**7**	**a. $\pi^2\delta^2\sigma^1$**	9.41
$Mn(BO)^-$	**6**	**a. $\pi^2\delta^2\sigma^1$**	**0.00**	$Mn(OB)^-$	**6**	**a. $\pi^2\delta^2\sigma^1$**	**-0.18**
$Fe(BO)^-$	3	a. $\pi^4\delta^2$	c	$Fe(OB)^-$	3	/	/
	5	**b. $\pi^2\delta^3\sigma^1$**	**0.00**		**5**	**b. $\pi^2\delta^3\sigma^1$**	**1.26**
$Co(BO)^-$	2	a. $\pi^4\delta^3$	1.88	$Co(OB)^-$	2	a. $\pi^4\delta^3$	22.59
	4	**b. $\pi^4\delta^3\sigma^1$**	**0.00**		**4**	**b. $\pi^4\delta^3\sigma^1$**	**20.71**
$Ni(BO)^-$	1	a. $\pi^4\delta^4$	92.87	$Ni(OB)^-$	1	a. $\pi^4\delta^4$	45.81
	3	**b. $\pi^4\delta^3\sigma^2$**	**0.00**		**3**	**b. $\pi^4\delta^3\sigma^2$**	**23.22**
$Cu(BO)^-$	**2**	**a. $\pi^4\delta^4\sigma^2$**	**0.00**	$Cu(OB)^-$	**2**	**a. $\pi^4\delta^4\sigma^2$**	**21.34**
$Zn(BO)^-$	**1**	**a. $\pi_d^4\delta_d^4\sigma_d^2$**	**0.00**	$Zn(OB)^-$	**1**	**a. $a'^2a''^2a'^2a''^2a'^2$**	**0.63**

Table S4. Relative energies (in kcal/mol) of the lowest lying state for MOB^- and MBO^- (M = Sc - Zn) complexes at the PBE, PBE0 and CCSD(T) levels of theory, respectively.

M	PBE		PBE0		CCSD(T)	
	MBO^-	MOB^-	MBO^-	MOB^-	MBO^-	MOB^-
Sc	0.00	-6.31	0.00	-7.6	0.00	-8.79
Ti	0.00	2.02	0.00	-0.03	0.00	-3.19
V	0.00	13.80	0.00	4.89	0.00	1.26
Cr	0.00	11.16	0.00	9.13	0.00	9.41
Mn	0.00	4.45	0.00	1.04	0.00	-0.18
Fe	0.00	7.97	0.00	3.84	0.00	1.26
Co	0.00	25.92	0.00	30.24	0.00	20.71
Ni	0.00	19.42	0.00	-15.89	0.00	23.22
Cu	0.00	24.80	0.00	21.88	0.00	21.34
Zn	0.00	2.74	0.00	2.02	0.00	0.63

Table S5. The electron configurations of $M(BO)^-$ and $M(OB)^-$ molecules at the PBE/TZ2P level, with geometric structures from CCSD(T)/def2-TZVP. The ground state species are highlighted in bold. Note: The italic electron configuration corresponds specifically to the occupancy of the metal's 3d orbitals.

$M(BO)^-$	2S+1	Valence Configuration	$M(OB)^-$	2S+1	Valence Configuration
$Sc(BO)^-$	2	$9\sigma^2 3\pi^4 10\sigma^2 11\sigma^2 1\delta^1$	**$Sc(OB)^-$**	**2**	**$9\sigma^2 3\pi^4 10\sigma^2 11\sigma^2 1\delta^1$**
$Ti(BO)^-$	**3**	**$9\sigma^2 3\pi^4 10\sigma^2 11\sigma^2 1\delta^2 4\pi^1$**	$Ti(OB)^-$	3	$9\sigma^2 3\pi^4 10\sigma^2 11\sigma^2 1\delta^1 4\pi^1$
$V(BO)^-$	**4**	**$9\sigma^2 3\pi^4 10\sigma^2 4\pi^2 1\delta^3 11\sigma^2$**	$V(OB)^-$	4	$9\sigma^2 3\pi^4 10\sigma^2 1\delta^1 4\pi^2 11\sigma^2$
$Cr(BO)^-$	**7**	**$9\sigma^2 3\pi^4 10\sigma^2 11\sigma^1 4\pi^2 1\delta^2 12\sigma^1$**	$Cr(OB)^-$	7	$9\sigma^2 3\pi^4 10\sigma^2 11\sigma^1 1\delta^2 4\pi^2 12\sigma^1$
$Mn(BO)^-$	6	$9\sigma^2 3\pi^4 10\sigma^2 1\delta^2 11\sigma^1 4\pi^2 12\sigma^2$	**$Mn(OB)^-$**	**6**	**$9\sigma^2 3\pi^4 1\delta^2 4\pi^2 10\sigma^1 11\sigma^2 12\sigma^2$**
$Fe(BO)^-$	**5**	**$9\sigma^2 3\pi^4 10\sigma^2 4\pi^2 1\delta^3 11\sigma^1 12\sigma^2$**	$Fe(OB)^-$	5	$9\sigma^2 3\pi^4 4\pi^2 10\sigma^1 1\delta^3 11\sigma^2 12\sigma^2$
$Co(BO)^-$	**4**	**$9\sigma^2 3\pi^4 10\sigma^2 11\sigma^1 4\pi^4 1\delta^3 12\sigma^1$**	$Co(OB)^-$	4	$9\sigma^2 3\pi^4 10\sigma^2 11\sigma^1 1\delta^3 4\pi^4 12\sigma^1$
$Ni(BO)^-$	**3**	**$9\sigma^2 3\pi^4 10\sigma^2 11\sigma^2 4\pi^4 1\delta^3 12\sigma^1$**	$Ni(OB)^-$	3	$9\sigma^2 3\pi^4 1\delta^3 10\sigma^2 4\pi^4 11\sigma^2 12\sigma^1$
$Cu(BO)^-$	**2**	**$9\sigma^2 3\pi^4 10\sigma^2 4\pi^4 11\sigma^2 1\delta^4 12\sigma^1$**	$Cu(OB)^-$	2	$9\sigma^2 3\pi^4 10\sigma^2 1\delta^4 4\pi^4 11\sigma^2 12\sigma^1$
$Zn(BO)^-$	**1**	**$1\delta^4 9\sigma^2 3\pi^4 10\sigma^2 4\pi^4 11\sigma^2 12\sigma^2$**	$Zn(OB)^-$	1	$11a'^2 3a''^2 12a'^2 4a''^2 13a'^2 14a'^2 15a'^2 5a''^2 16a'^2 17a'^2$

Table S6. T1 diagnostic values computed at the CCSD(T)/def2-TZVP level for the most stable monoboronyl complexes $M(BO)^-$/$M(OB)^-$ across the 3d series.

M	2s + 1	T1
$Sc(OB)^-$	2	0.035
$Ti(OB)^-$	3	0.030
$V(BO)^-$	4	0.045
$Cr(BO)^-$	7	0.025
$Mn(OB)^-$	6	0.024
$Fe(BO)^-$	5	0.030
$Co(BO)^-$	4	0.030
$Ni(BO)^-$	3	0.033
$Cu(BO)^-$	2	0.030
$Zn(BO)^-$	1	0.018

Table S7. The bond length (in Å) and bond angle (in °) and frequency (in cm^{-1}) of in $M(BO)^-$ and $M(OB)^-$ (M=Sc-Zn). Note that the slight nonlinearity reported for $Sc(OB)^-$ (179.8°) and $Mn(OB)^-$ (178.6°) are attributed to Jahn-Teller distortion with electrons occupying on the non-degenerated MOs.

Species	∠M-B-O	Length		Frequency		Species	∠M-O-B	Length		Frequency	
		M-B	B-O	O-B	B-M			M-O	O-B	O-B	O-M
$^2Sc(BO)^-$	180.0	2.58	1.23	1815	256	$^2Sc(OB)^-$	179.8	2.08	1.26	1615	413
$^3Ti(BO)^-$	180.0	2.41	1.23	1806	273	$^3Ti(OB)^-$	180.0	1.96	1.27	1586	473
$^6V(BO)^-$	180.0	2.27	1.23	1800	288	$^6V(OB)^-$	180.0	2.00	1.26	1657	397
$^7Cr(BO)^-$	180.0	2.29	1.23	1795	288	$^7Cr(OB)^-$	180.0	2.08	1.26	1677	313
$^6Mn(BO)^-$	180.0	2.42	1.23	1805	213	$^6Mn(OB)^-$	178.6	2.07	1.26	1653	301
$^3Fe(BO)^-$	180.0	2.26	1.23	1822	249	$^5Fe(OB)^-$	180.0	1.97	1.26	1652	350
$^2Co(BO)^-$	180.0	2.02	1.24	1767	339	$^4Co(OB)^-$	180.0	2.00	1.25	1691	305
$^1Ni(BO)^-$	180.0	1.96	1.24	1833	399	$^1Ni(OB)^-$	180.0	1.96	1.25	1694	327
$^2Cu(BO)^-$	180.0	1.98	1.23	1814	333	$^2Cu(OB)^-$	180.0	1.93	1.25	1693	318
$^1Zn(BO)^-$	179.9	2.51	1.24	1781	150	$^1Zn(OB)^-$	167.9	2.17	1.25	1657	196

Table S8. Atomic charges of M, BO^- ligands and bond orders of M-B and B-O bonds in $M(BO)^-$ (M = Sc - Zn)

Species	Mulliken Charge		Hirshfeld Charge		Mayer bond order	
	q(M)	q(BO^-)	q(M)	q(BO^-)	M-B	B-O
$^2Sc(BO)^-$	-0.52	-0.48	-0.49	-0.51	0.80	2.10
$^3Ti(BO)^-$	-0.55	-0.44	-0.45	-0.56	0.97	2.05
$^4V(BO)^-$	-0.59	-0.41	-0.48	-0.52	1.01	2.06
$^7Cr(BO)^-$	-0.46	-0.55	-0.37	-0.63	0.97	2.04
$^6Mn(BO)^-$	-0.54	-0.46	-0.48	-0.52	0.67	2.08
$^5Fe(BO)^-$	-0.41	-0.59	-0.39	-0.61	0.76	2.08
$^4Co(BO)^-$	-0.49	-0.51	-0.42	-0.58	1.19	1.98
$^3Ni(BO)^-$	-0.53	-0.47	-0.38	-0.62	1.05	2.01
$^2Cu(BO)^-$	-0.67	-0.33	-0.45	-0.55	1.11	2.05
$^1Zn(BO)^-$	-0.37	-0.63	-0.37	-0.63	0.39	2.03

Table S9. Theoretical charges of M, OB^- ligands and bond orders of M-B and B-O bonds in $M(OB)^-$ (M=Sc-Zn)

Species	Mulliken Charge		Hirshfeld Charge		Mayer bond order	
	q(M)	q(OB^-)	q(M)	q(OB^-)	M-O	O-B
$^2Sc(OB)^-$	-0.27	-0.73	-0.43	-0.57	0.43	1.61
$^3Ti(OB)^-$	-0.27	-0.73	-0.44	-0.56	0.53	1.57
$^4V(OB)^-$	-0.29	-0.71	-0.44	-0.56	0.49	1.60
$^7Cr(OB)^-$	-0.21	-0.79	-0.29	-0.71	0.35	1.67
$^6Mn(OB)^-$	-0.28	-0.72	-0.36	-0.64	0.37	1.60
$^5Fe(OB)^-$	-0.32	-0.68	-0.40	-0.60	0.44	1.58
$^4Co(OB)^-$	-0.24	-0.76	-0.31	-0.69	0.42	1.62
$^3Ni(OB)^-$	-0.33	-0.67	-0.31	-0.70	0.43	1.63
$^2Cu(OB)^-$	-0.30	-0.70	-0.33	-0.67	0.46	1.66
$^1Zn(OB)^-$	-0.26	-0.75	-0.25	-0.75	0.21	1.67

Table S10. The EDA-NOCV results for the $M(BO)^-$ (M = Sc–Zn) complexes at the PBE/TZ2P level. All the energies are given in kcal/mol. The table lists the total interaction energy (ΔE_{int}), Pauli repulsion (ΔE_{Pauli}), electrostatic interaction (ΔE_{elstat}), and orbital interaction (ΔE_{orb}), together with the σ- and π-components of ΔE_{orb} ($\Delta E_{orb\ \sigma}$ and $\Delta E_{orb\ \pi}$). Percentages in parentheses indicate the relative contributions of ΔE_{elstat} and ΔE_{orb} to the total attractive interactions ($\Delta E_{elstat} + \Delta E_{orb}$), and of

ΔE(kcal/mol)	Sc + $(BO)^-$	Ti + $(BO)^-$	V+ $(BO)^-$	Cr + $(BO)^-$	Mn + $(BO)^-$
fragments	Sc(δ^1) $BO^-(1\pi^4 5\sigma^2)$	Ti($\delta^1\pi^1$) BO^- $(1\pi^4 5\sigma^2)$	V($\pi^2\delta^1$) BO^- $(1\pi^4 5\sigma^2)$	Cr($\pi^2\delta^2\sigma^1$) BO^- $(1\pi^4 5\sigma^2)$	Mn($\pi^2\delta^2\sigma^1$) BO^- $(1\pi^4 5\sigma^2)$
ΔE_{int}	-49.69	-49.67	-63.21	-36.88	-36.09
ΔE_{Pauli}	92.82	115.47	139.50	111.97	110.95
ΔE_{elstat}	-85.69 (60.12%)	-102.71 (62.20%)	-127.86 (63.08%)	-105.58 (70.93%)	-91.87 (62.47%)
ΔE_{orb}	-56.83 (39.88%)	-62.43 (37.80%)	-74.85 (36.92%)	-43.27 (29.07%)	-55.17 (37.53%)
$\Delta E_{orb\ \sigma}$	-50.32 (88.54%)	-56.73 (90.87%)	-61.89 (82.69%)	-36.22 (83.71%)	-52.29 (94.78%)
$\Delta E_{orb\ \pi}$	-0.84 (1.48%)	-5.34 (8.56%)	-7.25 (9.69%)	-6.07 (14.03%)	-1.66 (3.01%)
ΔE(kcal/mol)	Fe + $(BO)^-$	Co + $(BO)^-$	Ni + $(BO)^-$	Cu + $(BO)^-$	Zn + $(BO)^-$
fragments	Fe($\pi^2\delta^3\sigma^1$) BO^- $(1\pi^4 5\sigma^2)$	Co($\pi^4\delta^3\sigma^1$) BO^- $(1\pi^4 5\sigma^2)$	Ni($\pi^4\delta^3\sigma^2$) BO^- $(1\pi^4 5\sigma^2)$	Cu($\pi^4\delta^4\sigma^2$) BO^- $(1\pi^4 5\sigma^2)$	Zn($\pi^4\delta^4\sigma^2$) BO^- $(1\pi^4 5\sigma^2)$
ΔE_{int}	-52.79	-59.90	-63.00	-56.62	-14.65
ΔE_{Pauli}	112.76	171.51	190.83	184.08	76.68
ΔE_{elstat}	-110.18 (66.55%)	-160.71 (69.21%)	-180.04 (70.65%)	-173.70 (72.16%)	-58.26 (63.79%)
ΔE_{orb}	-55.38 (33.45%)	-76.07 (30.79%)	-74.79 (29.35%)	-67.00 (27.84%)	-33.07 (36.21%)
$\Delta E_{orb\ \sigma}$	-43.20 (78.00%)	-46.53 (61.17%)	-51.95 (69.46%)	-57.30 (85.52%)	-29.48 (89.14%)
$\Delta E_{orb\ \pi}$	-2.64 (4.76%)	-17.02 (22.37%)	-13.62 (18.21%)	-9.49 (14.16%)	/ /

$\Delta E_{orb\ \sigma}$ and $\Delta E_{orb\ \pi}$ to ΔE_{orb}, respectively.

Table S11. The EDA-NOCV results for the $M(OB)^-$ (M = Sc–Zn) complexes at the PBE/TZ2P level. All energies are given in kcal·mol⁻¹. The table lists the total interaction energy (ΔE_{int}), Pauli repulsion (ΔE_{Pauli}), electrostatic interaction (ΔE_{elstat}), and orbital interaction (ΔE_{orb}), together with the σ- and π-components of ΔE_{orb} ($\Delta E_{orb\ \sigma}$ and $\Delta E_{orb\ \pi}$). Percentages in parentheses indicate the relative contributions of ΔE_{elstat} and ΔE_{orb} to the total attractive interactions ($\Delta E_{elstat} + \Delta E_{orb}$), and of $\Delta E_{orb\ \sigma}$ and $\Delta E_{orb\ \pi}$ to ΔE_{orb}, respectively.

ΔE(kcal/mol)	Sc + $(OB)^-$	Ti + $(OB)^-$	V+ $(OB)^-$	Cr + $(OB)^-$	Mn + $(OB)^-$
Interaction fragments	Sc(δ^1) $OB^-(1\pi^4 5\sigma^2)$	Ti($\delta^1\pi^1$) $OB^-(1\pi^4 5\sigma^2)$	V($\pi^2\delta^1$) $OB^-(1\pi^4 5\sigma^2)$	Cr($\pi^2\delta^2\sigma^1$) $OB^-(1\pi^4 5\sigma^2)$	Mn($\pi^2\delta^2\sigma^1$) $OB^-(1\pi^4 5\sigma^2)$
ΔE_{int}	-55.71	-49.59	-54.15	-25.21	-31.66
ΔE_{Pauli}	116.81	142.62	110.47	81.47	100.62
ΔE_{elstat}	-99.61	-111.79	-93.84	-65.62	-79.41
	(57.74%)	(58.17%)	(57.00%)	(61.51%)	(60.03%)
ΔE_{orb}	-72.92	-80.38	-70.78	-41.06	-52.87
	(42.26%)	(41.83%)	(43.00%)	(38.48%)	(39.97%)
$\Delta E_{orb\ \sigma}$	-53.68	-61.59	-53.68	-31.24	-42.75
	(73.61%)	(76.62%)	(75.84%)	(76.08%)	(80.86%)
$\Delta E_{orb\ \pi}$	-12.79	-15.75	-19.34	-7.88	-7.29
	(17.53%)	(19.59%)	(27.32%)	(19.19%)	(13.79%)
ΔE(kcal/mol)	Fe + $(OB)^-$	Co + $(OB)^-$	Ni + $(OB)^-$	Cu + $(OB)^-$	Zn + $(OB)^-$
Interaction fragments	Fe($\pi^2\delta^3\sigma^1$) $OB^-(1\pi^4 5\sigma^2)$	Co($\pi^4\delta^3\sigma^1$) $OB^-(1\pi^4 5\sigma^2)$	Ni($\pi^4\delta^3\sigma^2$) $OB^-(1\pi^4 5\sigma^2)$	Cu($\pi^4\delta^4\sigma^2$) $OB^-(1\pi^4 5\sigma^2)$	Zn($\pi^4\delta^4\sigma^2$) $OB^-(1\pi^4 5\sigma^2)$
ΔE_{int}	-45.14	-33.67	-39.83	-31.03	-11.70
ΔE_{Pauli}	90.67	75.65	78.47	96.48	60.11
ΔE_{elstat}	-81.97	-63.30	-70.36	-78.15	-44.16
	(60.36%)	(57.90%)	(59.48%)	(61.28%)	(61.50%)
ΔE_{orb}	-53.84	-46.02	-47.94	-49.37	-27.64
	(39.64%)	(42.10%)	(40.52%)	(38.72%)	(38.50%)
$\Delta E_{orb\ \sigma}$	-33.52	-30.37	-34.06	-41.61	-23.76
	(62.26%)	(65.99%)	(71.05%)	(84.28%)	(85.96%)
$\Delta E_{orb\ \pi}$	-8.24	-4.79	-5.34	-4.17	-2.94
	(15.30%)	(10.41%)	(11.13%)	(8.47%)	(10.64%)

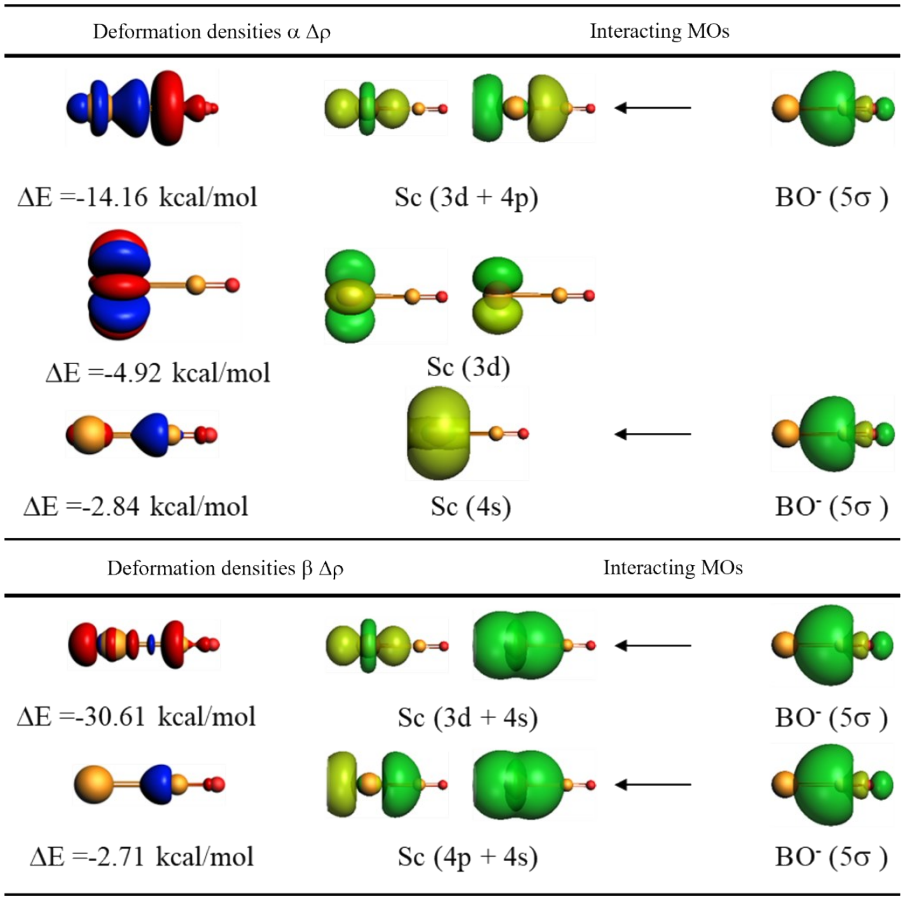

Figure S3. The deformation densities Δρ of the most important pairwise orbital interactions (ΔE_{orb}) of $ScBO^-$ between Sc (…$3d^1 4s^2$) and BO^- (…$1\pi^4\ 5\sigma^2\ 2\pi^0$) at the PBE/TZ2P level. The direction of the charge flow is from red to blue.

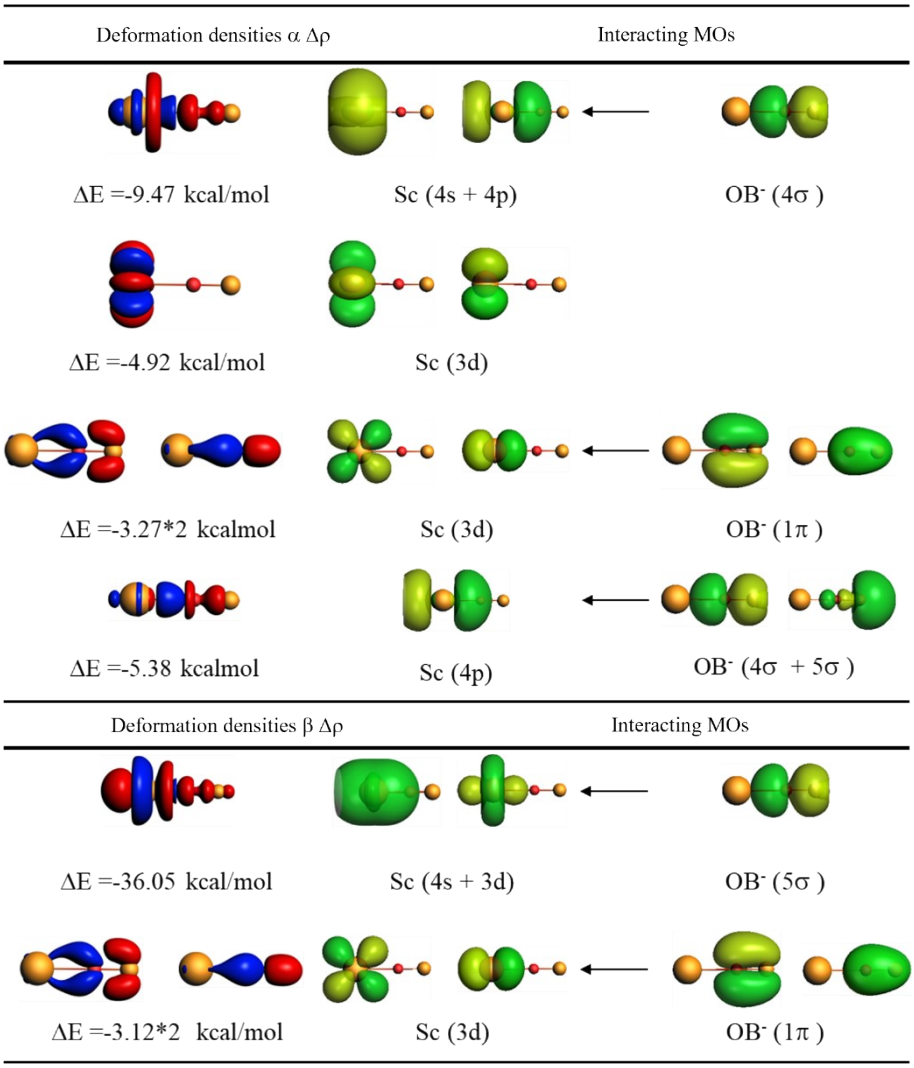

Figure S4. The deformation densities Δρ of the most important pairwise orbital interactions (ΔE_{orb}) of $ScOB^-$ between Sc (…$3d^1 4s^2$) and OB^- (…$1\pi^4\ 5\sigma^2\ 2\pi^0$) at the PBE/TZ2P level. The direction of the charge flow is from red to blue.

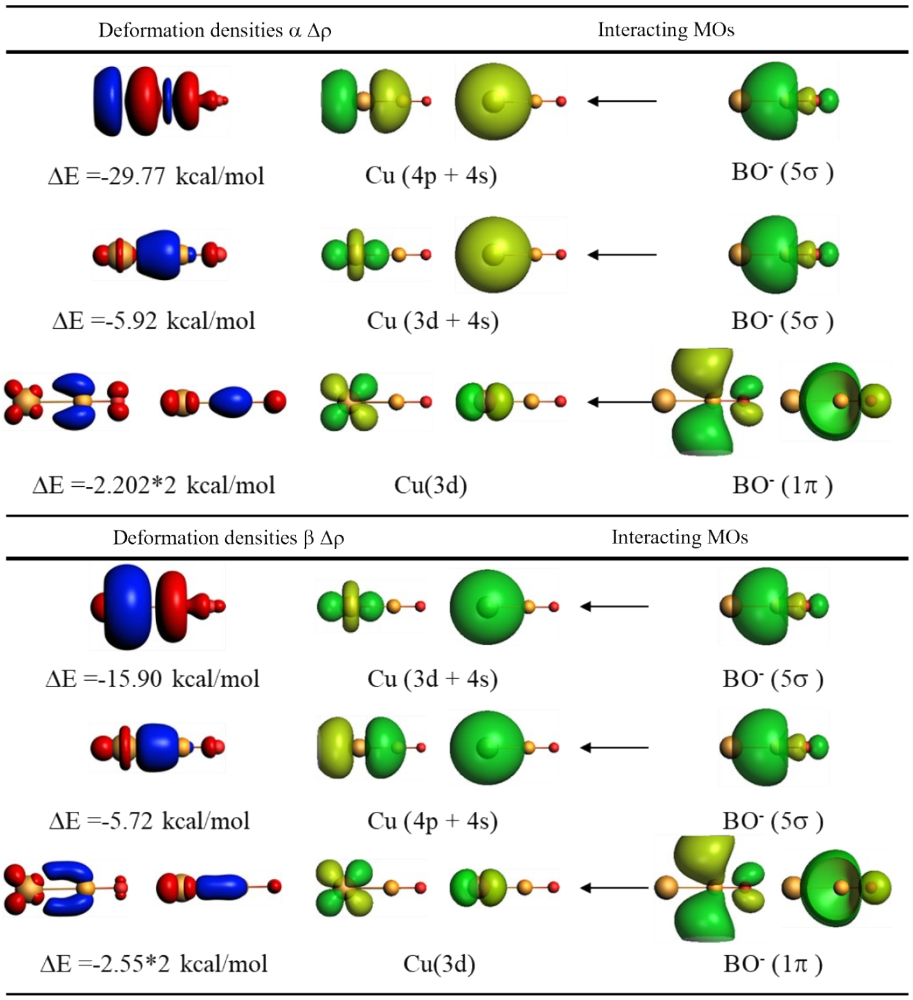

Figure S5. The deformation densities Δρ of the most important pairwise orbital interactions (ΔE_{orb}) of $CuBO^-$ between Cu(…$3d^{10}4s^1$) and BO^- (…$1\pi^4\ 5\sigma^2\ 2\pi^0$) at the PBE/TZ2P level. The direction of the charge flow is from red to blue.

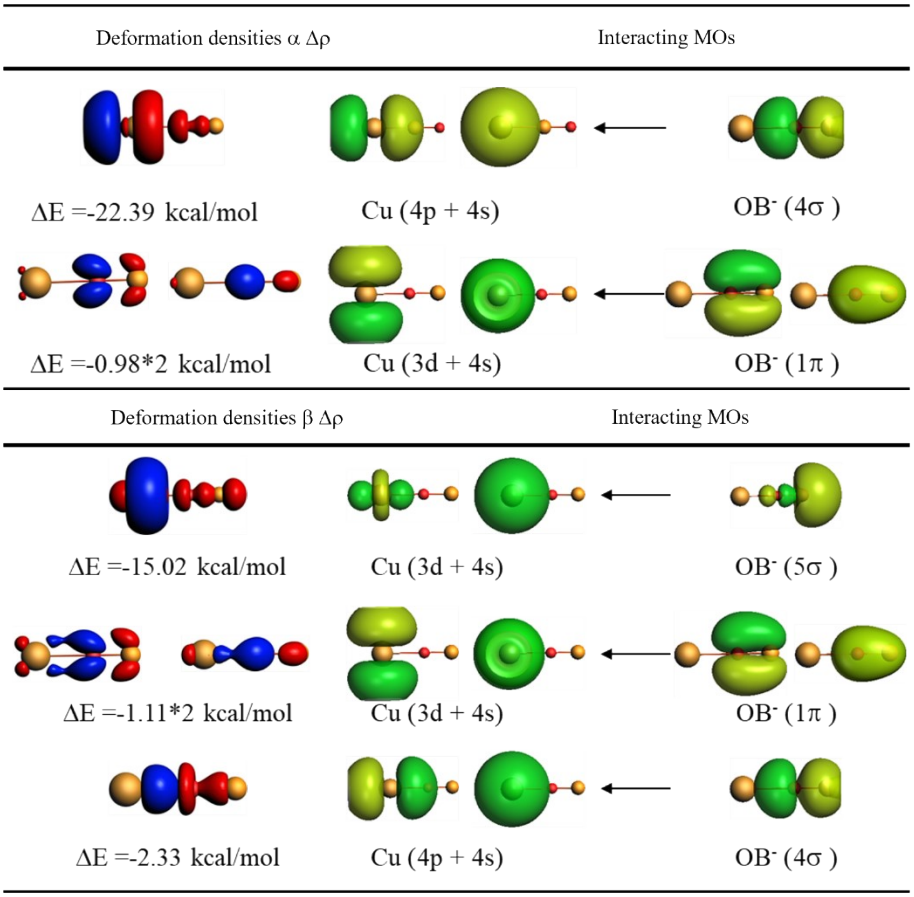

Figure S6. The deformation densities Δρ of the most important pairwise orbital interactions (ΔE_{orb}) of $CuOB^-$ between Cu(…$3d^{10}4s^1$) and OB^- (…$1\pi^4\ 5\sigma^2\ 2\pi^0$) at the PBE/TZ2P level. The direction of the charge flow is from red to blue.

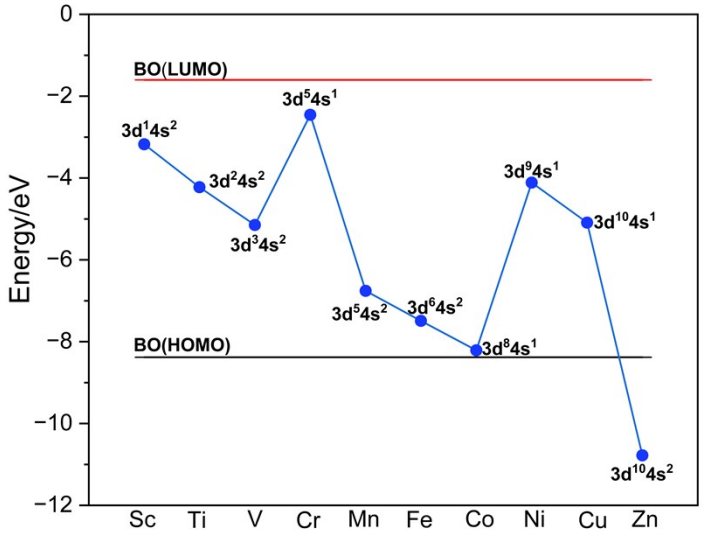

Figure S7. The molecular orbital (MO) energies of the BO^- frontier molecular orbitals (HOMO and LUMO) and the 3d orbitals of transition metals M (Sc–Zn), illustrating how the metal(3d) energy stabilization governs metal–ligand interaction trends.

Table S12. Relative energies (in kcal/mol) of the lowest-lying species for MOB^- and MBO^- (M=Ni, Pd, Pt) complexes at the PBE, PBE0 and CCSD(T) levels of theory, respectively.

M	PBE		PBE0		CCSD(T)	
	$-BO^-$	$-OB^-$	$-BO^-$	$-OB^-$	$-BO^-$	$-OB^-$
Ni	0.00	19.42	0.00	-15.89	0.00	22.99
Pd	0.00	55.41	0.00	50.90	0.00	54.95
Pt	0.00	80.84	0.00	77.79	0.00	79.48

Table S13. The EDA-NOCV results for the MBO^- (M=Ni, Pd, Pt) complexes at the PBE/TZ2P level. All energies are given in kcal·mol^{-1}. The table lists the total interaction energy (ΔE_{int}), Pauli repulsion (ΔE_{Pauli}), electrostatic interaction (ΔE_{elstat}), and orbital interaction (ΔE_{orb}), together with the σ- and π-components of ΔE_{orb} ($\Delta E_{orb\ \sigma}$ and $\Delta E_{orb\ \pi}$). Percentages in parentheses indicate the relative contributions of ΔE_{elstat} and ΔE_{orb} to the total attractive interactions ($\Delta E_{elstat} + \Delta E_{orb}$), and of

ΔE(kcal/mol)	$Ni(BO)^-$	$Pd(BO)^-$	$Pt(BO)^-$
Interaction fragments	Ni($\pi^4\delta^3\sigma^2$) $BO^-(1\pi^4 5\sigma^2)$	Pd($\pi^4\delta^4\sigma^2$) $BO^-(1\pi^4 5\sigma^2)$	Pt($\pi^4\delta^4\sigma^1$) $BO^-(1\pi^4 5\sigma^2)$
ΔE_{int}	-63.00	-84.55	-129.98
ΔE_{Pauli}	190.83	322.54	446.81
ΔE_{elstat}	-180.04 (70.65%)	-325.55 (79.97%)	-430.10 (74.57%)
ΔE_{orb}	-74.79 (29.35%)	-81.54 (20.03%)	-146.69 (25.43%)
$\Delta E_{orb\ \sigma}$	-51.95 (69.46%)	-55.18 (67.67%)	-104.94 (71.54%)
$\Delta E_{orb\ \pi}$	-13.62 (18.21%)	-26.02 (31.91%)	-38.34 (26.14%)

$\Delta E_{orb\ \sigma}$ and $\Delta E_{orb\ \pi}$ to ΔE_{orb}, respectively.